Preliminary steps in the analysis of the protective potential of plant extracts against SARS-CoV-2 infection in lung cells

Andrina Chambers

Instituto de Biomedicina y Biotecnología de Cantabria (IBBTEC)

Dr. Ana Villar Ramos (Director) Dr. Ana Palanca (Codirector)

English

14th June 2021

Table of Contents

Abstract

The SARS-CoV-2 pandemic is without doubt one of the greatest challenges modern medicine has ever faced. To date there is still no cure and effective treatments are desperately required to combat both the viral infection and the wide variety of consequent pathologies displayed in COVID-19 patients. One of the most severe pathologies seen in patients with COVID-19 is pulmonary fibrosis resulting from the cytokine storm generated, which activates fibroblasts leading to the progressive accumulation of collagen fibres in the lungs. Pulmonary fibrosis compromises lung function and can ultimately lead to respiratory failure. Type II pneumocytes (ATII) are particularly susceptible to Sars-CoV-2 infection. ATII cells are responsible for the production of surfactant Protein C (SPC) and other surfactant components fundamental to lung integrity. In this study ATII cells were isolated from non-covid patient´s lungs and characterized by a specific enzymatic test. The expression of SPC in ATII cells was tested under different conditions mimicking those of COVID-19 disease.

Many plants possess a variety of secondary metabolites with antibiotic, antifungal and antiviral properties and are the basis for many traditional and modern medicines. In this study, we analysed the effect of different plant extracts from *Marchantia* and *Arabidopsis* mutants on SPC expression in the presence of Transforming Growth Factor β (TGF- β) as a representative cytokine of the cytokine storm.

Preliminary results indicated that some of the tested plant extracts could provide some protection against a reduction in SPC expression in conditions mimicking the cytokine storm in COVID-19 disease.

Introduction

Coronavirus disease 2019 (COVID-19) is an ongoing pandemic which first appeared in December 2019 in Wuhan city of the Hubei province in China. The disease rapidly spread globally and to date has infected over 176 million people and caused 3.81 million deaths (*1*). It is caused by a novel Betacoronavirus, known as severe acute respiratory syndrome coronavirus 2 (SARS-CoV-2) (*2*). SARS-CoV-2 primarily affects the respiratory system, similar to the previous coronavirus outbreaks of severe acute respiratory syndrome (SARS) and Middle East respiratory syndrome (MERS) (*3*). Infection can be asymptomatic or present only mild symptoms, commonly similar to those of seasonal flu, however in some cases can cause systemic hyperinflammation, pulmonary fibrosis, lung collapse, multi-organ dysfunction, and death (*4*). Various vaccines against the virus have been developed at an unprecedented rate however there is still an urgent need for focusing research and funding into the development of novel treatments for SARS-CoV-2 infected patients to reduce mortality and to treat the resulting pathologies caused.

Viral entry

The virus enters the respiratory tract where the viral surface spike (S) glycoprotein binds to angiotensin-converting enzyme 2 (ACE2) receptors of epithelial cells, particularly Type II Alveolar Epithelial Cells (ATII) (*5*). SARS-CoV-2 uses the same receptor as its main point of entry as SARS-Co-V but has a higher binding affinity, thought to increase transmission ability (*5*). Proteolytic cleavage of the S protein, by both Transmembrane Protease Serine 2 (TMPRSS2) and Furin proteases, is required to enable viral cell entry (*5*). Furin is ubiquitously expressed whereas TMPRSS2 and ACE2 are co-expressed within nasal epithelial cells and in ATII cells within the lungs and bronchial branches, which explains some of the tissue tropism of SARS-CoV-2 (*5*).

Infection and cytokine storm

SARS-CoV-2 generally infects the upper respiratory track and symptoms typically include fever, headache, and cough. As the virus starts replicating and migrating down the airways, it is detected by pathogen recognition receptors of immune cells triggering the innate immune system and the release of cytokines and chemokines (*6*). These are responsible for initiating a complex system of signalling thereby inducing inflammation, the recruitment of more immune cells and activation, proliferation, and cell differentiation of innate and adaptive responses (*6*). The major cytokines produced are Interleukin (IL)-1α/β, IL-18 and IL-6, tumour necrosis factor (TNF)-α, Interferon (IFN)-α/β and Transforming growth factor (TGF)-β; while the major chemokines produced are Monocyte Chemoattractant Protein (MCP)-1, MCP-3, Macro-phage Inflammatory Protein (MIP-1-α), CCL-5 (Chemokine (C-C motif)

ligand 5) and IFN-γ-inducible protein-10 (IP-10) (*6*). Severe cases have been attributed to a maladaptive or imbalanced immune response with chronic, exacerbated cytokine release and apoptosis of epithelial and endothelial cells, followed by vascular leakage and an abnormal T cell and macrophage response (*6*). The virus also has various mechanisms for avoiding or delaying detection thereby increasing viral load and facilitating progression to the lower respiratory airways and infecting the alveolar space where gas exchange takes place causing pneumonia which can lead to inflammatory-induced acute lung injury and acute respiratory distress syndrome (ARDS) (*5*).

In most moribund patients, a cytokine storm can be observed, characterized by high serum concentrations of IL 1, 6, 8 and 10, TNF-α, granulocyte colony-stimulating factor, MCP-1, MIP-1-α, and IP-10 and can eventually lead to multiple organ failure (*7, 8*). The hyperactive inflammatory state caused by the cytokine storm in severe cases of SARS-CoV-2 infection, and the elevated levels of the growth factors and cytokines TGF-β, Il-6, and TNF-α, are most likely the main causes of pulmonary fibrosis (*4*).

Type II Alveolar Epithelial Cells (ATII)

The pulmonary alveolar epithelium is composed of two types of differentiated epithelial cells:

Alveolar type 1 (ATI) cells which account for 85-90% of all alveolar cells and are responsible for mediating gas exchange and alveolar type 2 (ATII) cells which account for 10-15% and are responsible for the production and secretion of surfactant components which reduce the superficial tension of fluid inside alveoli (*5*). Surfactant is a thin aqueous film coating the surface of the alveolar and its tension reducing function comes from interaction between phospholipids and two hydrophobic proteins, surfactant protein B (SPB) and surfactant protein C (SPC)(*9*). The reduction in superficial tension prevents alveolar collapse and is fundamental to lung integrity (*5*). SPC also plays a role in maintaining alveolar epithelial homeostasis abnormal expression of SPC is seen in the development of lung disease and microbial pulmonary infection(*9*). ATII cells also play fundamental roles in immune defence and regeneration during and following lung injury (*5*). They are the progenitors of ATI cells and therefore have the capacity for both self-renewal and differentiation to ATI cells (*5*). As ATII cells co-express TMPRSS2 and ACE2 enabling viral entry, these cells are particularly susceptible to Sars-CoV-2 infection (*10*). ATII cells are being infected and dying therefore secretion of surfactant components is decreased, and the fluid tension rises creating a stickiness (*10*). The increased stickiness leads to a reduction in gas exchange, and further contributes to the uncontrolled inflammation brought about by the innate immune response leading to collapsing of alveoli and ARDS (*10*).

SARS-CoV-2 and pulmonary fibrosis

Pulmonary fibrosis is commonplace following severe and/or persistent lung damage from a variety of causes such as respiratory infections, connective tissue disorders, chronic granulomatous diseases or

medications (*3*). Clinical, radiographic and autopsy reports show this was also the case following SARS and MERS infection (*3*). Some patients who had previously been infected with SARS or MERS were found to have residual pulmonary fibrosis two years after hospital discharge (*11*). Following recovery from COVID-19, many patients who had suffered from ARDS or severe pneumonia were found to have pulmonary fibrosis (*12*). One study, assessing 284 hospitalized patients who achieved a clinical cure, found that pulmonary fibrosis occurred in 100% of patients suffering from severe or critical COVID-19 and in 84.15% of total hospitalized patients (*11*). The results also indicated that patients suffering from moderate COVID-19 predominantly develop mild-to-moderate pulmonary fibrosis whereas patients suffering with critical COVID-19 mainly develop severe fibrosis (*11*). Pathological manifestations of COVID-19 strongly resemble those of SARS and MERS however, whether or not it can cause irreversible pulmonary fibrosis needs more investigation (*11*). As in previous coronavirus outbreaks, SARS-CoV-2 can also induce an excessive, aberrant and non-effective immune response leading to severe inflammation initiating a profibrotic response (*12*). For those who survive intensive care, excessive and prolonged cytokine overexpression can cause long-term lung damage, including fibrosis that could promote lung function decline, a significant reduction in quality of life and, in severe cases, is associated with increased mortality (*7*).

Fibrosis is a pathophysiological condition characterized by excessive production and deposition of extracellular matrix (ECM) proteins causing scarring of the tissue (*13*). The ECM provides a scaffold for residing cells within a tissue or organ as well as mediating certain cellular functions such as adhesion, migration, proliferation, and differentiation (*5*). ECM composition varies between tissues but is primarily composed of collagens while also contains elastic fibres, fibronectin, laminins, proteoglycans and glycosaminoglycans (*5*). Fibrosis is due to a maladaptive or disordered wound healing as a result of injury or disease, this is initially a protective mechanism that attempts to preserve structure and function and can be beneficial for healing and tissue regeneration however, when damage is severe or persistent there is an excessive or continuous accumulation of ECM components, resulting in fibrosis (*13*). Pulmonary fibrosis remodels tissue architecture causing a thickening and stiffening of the tissue around and between the alveoli thereby impairing lung function and can ultimately result in organ failure (*11*). The mechanisms responsible for the pathogenesis of fibrosis are complex and involve interplay between pro-fibrotic cells, growth factors and pro-inflammatory cytokines (*14*). A key step leading to fibrosis is the activation of fibroblasts which induces them to proliferate and differentiate into myofibroblasts which in turn secrete significant amounts of ECM proteins and adopt a contractile phenotype similar to that of smooth muscle tissue (*15*). Transforming growth factor beta (TGF-β) is the best characterized fibrogenic growth factor and considered the most important cytokine implicated in the recruitment and activation of fibroblasts in response to chronic injury. TGF-β signalling is initiated when TGF-β binds to form a complex with the transmembrane serine/threonine kinase receptors TGF-βRI and TGF-βRII, leading to the activation of a cascade of intracellular mediators (*16*). The canonical pathway induced by TGF-β involves Smad proteins whereby the active receptor complex

phosphorylates Smad2 or Smad3 propagating the signal (*16*). Smad2/3 can then form a complex with Smad4 which translocate to the nucleus to initiate a transcriptional response resulting in ECM synthesis (*16*).

Vaccines and treatments

No specific anti-viral treatment exists against SARS-CoV-2 (*7*). Clinical treatment is mainly limited to symptomatic treatment and organ support in intensive care from patients with COVID-19 (*7*). Since the beginning of the outbreak, governments and global public health bodies have mainly focused on preventing the viruses spread and the development of vaccines, but as infection rates have remained very high in some countries, more effective treatments are desperately needed to combat the virus and the large array of symptoms exhibited, thereby reducing mortality and long-term health effects of COVID-19. The current vaccination efforts are providing promise for a considerable reduction in cases, however, there remains a high possibility that the virus won´t ever be eradicated and the emergence of new strains risk rendering current vaccines ineffective therefore further highlighting the need for novel therapeutics. An anti-fibrotic treatment administered to patients with an ongoing SARS-CoV-2 infection could prevent deterioration of the clinical situation, in some cases preventing mortality, and also prevent residual pulmonary fibrosis following recovery thereby preventing long-term lung function impairment (*4*). Some potential therapeutic strategies could be based on the protection of ATII cell homeostasis to prevent cytokine storm-produced fibrosis.

Telomeres

Cell homeostasis requires the presence of a certain length of telomeres in cells to enable the healthy reproduction and repopulation of cells (*17*). Telomeres are nucleoprotein complexes located at the ends of chromosomes comprising of a region of repetitive nucleotide sequence and are essential for chromosome protection and genomic integrity (*18*). In vertebrates, telomeres are comprised of tandem repeats of the DNA sequence TTAGGG bound to the six-subunit protein complex known as shelterin which enables the cell to distinguish chromosome ends from DNA damage (*18*). One of the molecular pathways underlying aging is the progressive shortening of telomeres leading to a reduced proliferation potential of somatic cells (*17*). This can in-turn cause an increased pressure on proliferating cells, such as stem cells and immune cells, to divide more, in order to maintain cell populations within tissues (*17*). Cellular stress due to viral infection or other causes can also necessitate repetitive cell division accelerating the aging process and telomere shortening (*17*). Telomeres become progressively shorter with subsequent cell divisions due to the end replication problem where-by the ends of linear DNA of the lagging strand, previously occupied by the RNA primer, cannot be replicated completely during DNA synthesis (*18*). Telomeres progressively shorten with increasing age and, when they become critically short, can lead to genomic instability, cellular senescence or apoptosis, and loss of the

regenerative capacity of tissues (*18*). Lung function is progressively impaired with age leading to an increased risk of developing pulmonary disease, lung cancer or idiopathic pulmonary fibrosis (*18*). Telomerase is a reverse transcriptase able to elongate telomeres thereby compensating telomere shortening with age (*18*). It is active in most proliferating cells though its expression is silenced in the majority of somatic cell types after birth (*18*). In the lungs, telomeres of patients with idiopathic pulmonary fibrosis are reported to be shorter than those of healthy individuals (*18*). Inducing telomere dysfunction in ATII cells in mice was sufficient to induce pulmonary fibrosis (*18*). Telomerase-deficient and wild-type mice with short telomeres in their lung cells, were treated with bleomycin. Bleomycin is primarily used is as an antitumor antibiotic for various carcinomas and lymphomas and pulmonary fibrosis is a well-known side effect so it is widely used in experimental models for lung fibrosis (*19*). This treatment induced fibrosis in telomerase-deficient mice, but not in wild-type mice (*18*). Furthermore, treating these mice with telomerase gene therapy, in order to activate telomerase in the lung cells, thereby elongating telomeres, was able to prevent the progression of fibrosis (*18*). Moreover, aging also leads to a decrease in proliferation of ATII cells, a phenomenon that is observed earlier in telomerase-deficient mice, implying that cells with short or dysfunctional telomeres have a reduced capacity for regeneration of tissue (*18*). It has been found that patients with shorter telomeres are at a higher risk of developing severe COVID-19 pathologies (*17*). It has been hypothesized that the need for rapid cellular regeneration caused by SARS-CoV-2 infection, and the reduced capacity for patients with short telomeres to fulfil this demand, could be exhausting the regeneration potential of the lungs therefore contributing to fibrosis (*17*). Thus, telomere length and maintenance could serve as a prognosis for which patients are more likely to suffer from pulmonary fibrosis and a reduced ATII regeneration capacity, as a result of COVID-19. It is unknown though if shortened telomeres are a cause or an effect of severe COVID-19 pathology.

Plant extracts

Plants have been known to display an array of medicinal properties and have been used in traditional medicines for thousands of years. Many modern medicines are derived from the numerous chemical compounds medicinal plants produce. There are two main categories of phytochemicals produced by plants: Primary and secondary metabolites. Primary metabolites are directly involved in growth, development and reproduction and therefore similar across species (*20*). Secondary metabolites are not essential for basic life functions and are generally compounds that confer a selective advantage to the organism such as protection against biotic or abiotic stresses (*21*). Some possess antibiotic, antifungal and antiviral properties enabling them to protect plants from pathogens (*22*). Secondary metabolites are an abundant source of novel compounds with potential pharmaceutical applications and their biological properties as well as strategies for their targeted expression and purification are very active fields of research (*23*).

Many plants are also able to live for hundreds of years and show distinct telomere maintenance features compared to humans such as indefinitely proliferating meristems, reversible regulation of telomerase in somatic cells and an absence of developmental telomere shortening (*24*).

Two extremely well established and popular biological plant models are *Arabidopsis* and *Marchantia*. *Arabidopsis* is a popular model organism in plant biology and the first plant to have its genome sequenced (*21*). More papers are published on *Arabidopsis* each year than on each of Saccharomyces, Caenorhabditis, Zebrafish, Chicken, or Drosophila and it has largely contributed to our understanding of plant development, signalling, hormone biology, pathogen defence, disease resistance, and abiotic stress response (*25*). A large variety of mutant lines of *Arabidopsis* exist, facilitating genetic and physiological analysis and over expression of various secondary metabolites (*21*). Additional advantages to research include its relatively short generation time, small size, diploid genetics and its high number of offspring (*21*). *Marchantia* is a dioecious liverwort found in most temperate climates and known for its ample range of biologically active compounds (*26*). It has been mentioned in ancient Greek texts as a plant used to prevent infection and inflammation of open wounds. Its physiological and morphological changes in response to environmental changes have been studied intensely for almost 200 years (*26*). Like *Arabidopsis*, *Marchantia* is another popular model organism in plant biology pertaining the advantages of having had its relatively small, haploid genome sequenced as well as having a short life cycle, ease of propagation and crossing and a high frequency of transformation (*26*). Both plants are also of high interest for their potential to produce phytopharmaceutical and nutraceutical substances or pharmaceutical proteins (*21, 26*).

Other studies have found plant extracts that can ameliorate bleomycin-induced pulmonary fibrosis and work in synergy with bleomycin to enhance its anti-cancer activity(*27*). We hypothesise that by protecting ATII cells, this would prevent or reduce the cytokine storm and therefore fibroblasts would not be activated, so resulting fibrosis would be reduced. This study will be preparing the conditions required for screening various *Arabidopsis* and *Marchantia* plant extracts for possible natural protective properties in ATII cells, in an environment that recreates the cytokine storm caused by SARS-CoV-2. Moreover, we will take preliminary steps to enable telomere measurement in human ATII cells under screening conditions.

Objectives

With the overall objective of finding potential plant extract candidates for the prevention or reduction of fibrosis in SARS-CoV-2 infection, the objectives of this research are the following:

1: To Extract and purify ATII cells from clinical lung samples and confirm their purity enzymatically.

2: To establish cell viability over a 24-hour period to enable treatment in ATII cells and establish the number of cells required to yield sufficient quantities of RNA to allow for retro-transcription and detection of surfactant protein C (SPC).

3: To Analyse the effect of TGF-β in ATII cells on SPC gene expression.

4: Establish optimal culture conditions that allow measurement of telomere length via HTQ-FISH techniques in ATII cells.

5: Determine the effect of total metabolites of 4 plant extracts from *Marchantia* and total 4 plant extracts from *Arabidopsis* on SPC expression in ATII cells.

6: To establish the optimal conditions for SARS-CoV-2 infection of ATII cells.

7: To Isolate and culture primary human fibroblasts from clinical lung samples obtained from biopsies for future experiments.

Methods

This project was approved by the bioethics committee of the Hospital de Valdecilla and by the biosafety and bioethics committees of the Institute of Biomedicine and Biotechnology of Cantabria. All patients have signed their informed consent to take part in this study. Lung sections are used from patients with cancer, who undergo lung surgery to remove the tumour. The lung section is the one furthest away from the tumour.

Isolation of human ATII cells from clinical lung samples

Preparation of solutions:
Physiological saline 0.9% NaCl 0.15M
Trypsin (T8003-1G) 2.5 mg per 1 ml Hank′s Balanced Salt Solution (HBSS)
DNase 1(10104159001): 250 µg per 1 ml HBSS
DNase 2 solution: 100 µg per 1 ml HBSS
Cell culture medium: Dulbecco's Modified Eagle Medium supplied by Sigma-Aldrich RPMI-1640, supplemented with 10% Foetal Bovine Serum (FBS), 1% penicillin-streptomycin and 1% antifungal agent Amphotericin B all supplied by Gibco.

NaCl 0.2%

NaCl 1.6%

All solutions were either autoclaved or filtered through a 0.2 µm filter from Minisart.

In a safety cabinet, samples extracted from patient lungs were washed with physiological saline using a syringe and needle until tissue acquired a grey colour and contained less than 1 x 10^4 monocytes/ml. Tissue was infused with 10-15 ml of trypsin using a syringe and needle until the tissue was inflated. Samples were incubated at 37ºC for 15 minutes. This process was repeated 3 times replacing the trypsin each time. Trypsin was eliminated and samples were cut until blended in the presence of 10ml FBS. Samples were transferred to a 50ml falcon and 7ml DNase 1 was added. Solutions were shaken vigorously for 5 minutes then filtered a 400-500 µm gauze followed by a 40 µm one. The filtrates were centrifuged at 520 xg for 20 minutes at 12ºC the cell pellets resuspended in 30 ml of DNase II solution. The average number of nucleated cells was determined using a hemacytometer and 500 µl sample was taken to perform a cytocentrifuge. Solutions were then incubated on a 150mm tissue culture dish for 2 hours at 37ºC to eliminate macrophages and adhesive cells. Cell suspension was centrifuged at 520 xg for 20 minutes at 12ºC and cell pellets resuspended in 10ml DMEM. The average cell number was determined using a haemocytometer and a second sample of 500 µl was taken to perform a cytocentrifuge. Cells were then either resuspended in cell culture medium and plated or frozen in cell culture medium containing 10% DMSO. To proceed with experimental work using frozen ATII cells, cells were defrosted by warming the vial of frozen cells in a water bath at 37ºC for 1 minute, then adding 1 ml of physiological saline drop by drop while swirling continually. Cells were centrifuged for 10 minutes at 500 xg and resuspended in cell culture medium.

Alkaline phosphatase histochemical staining of ATII cells

Purity of ATII cell extractions were measured enzymatically using the Leukocyte Alkaline Phosphatase Kit based on naphthol AS-BI and fast red violet LB by Sigma. Cell samples taken during ATII extractions were cytocentrifuged onto a microscope slide.

Diazonium salt solution was prepared by adding 1 ml sodium nitrate solution to 1 ml of FRV-Alkaline solution and gently inverted and left to stand for 2 minutes. The solution was added to 45 ml of deionized water at room temperature. 1 ml of Naphthol AS-BI Alkaline Solution was added, the solution was mixed and added to a Coplin jar. Slides were fixed by immersing them in Citrate-Acetone-Formaldehyde Fixative at room temperature for 30 seconds then rinsed gently in deionized water for 45 seconds. Slides were subsequently added to the alkaline-dye mixture described above and incubated at room temperature for 30 minutes while protecting immersed slides from direct light. Slides were removed from the Coplin jar and rinsed for 2 minutes in deionized water. They were counterstained for 2 minutes with Hematoxylin Solution, rinsed under tap water and allowed to air dry. Slides were mounted using DPX Mountant from Sigma and samples were digitalized with the AxioScan.Z1 slide

scanner (Zeiss). Slides were scanned with a x10/NA 0.55 Plan-APO objective (0.442 mm/px) and a HV-F201 colour camera with a 1600x1200 pixels sensor and a high-resolution mosaic was exported as jpg. White balance, camera exposure time and image brightness were adjusted to maximize colour fidelity and contrast. Images were analysed by selecting 4 zoomed sections of each image and quantifying the total number of nucleated cells versus the number of pink-purple alkaline phosphatase positive ATII cells, and the percentage of ATII cells was calculated by taking the mean of 4 measurements per sample.

ATII cell viability over a 24-hour period

Cells were defrosted and the initial cell number of alive and dead cells were established using a haemocytometer and by staining dead cells with trypan blue from Gibco. Cells were seeded 100,000 alive cells per well in 400 µl of cell culture medium on a 24 well plate. After 12 hours of incubation at 37ºC, both alive and dead cells were counted by taking a sample of the supernatant. At 24 hours, the supernatant was collected, attached cells were detached by incubating with 1 ml trypsin-EDTA solution from Sigma for 3 minutes and added to the supernatant. Cells were centrifuged at 500 xg for 10 minutes and resuspended in the initial volume of 400 µl of cell culture medium. The number of dead and alive cells were counted again using a haemocytometer.

Seeding and treating ATII cells

Cells were counted using a haemocytometer, resuspended in cell culture medium to the required concentration, seeded into cell culture dishes and incubated for 2 hours at 37ºC. All treatments and/or infections were performed 2 hours after seeding cells and incubated for a further 24 hours at 37ºC before being prepared for RNA isolation, or fixation to allow telomere measurement via HTQ-FISH.

Preparation for RNA isolation

To isolate RNA from ATII cells directly after they had been defrosted, the cells were centrifuged at 500 xg for 10 minutes, their supernatants were discarded, and the cell pellets were resuspended in 800 µl NZYol (MB18501) from Nzytech. RNA was immediately extracted according to the RNA extraction protocol outlined below.

To isolate RNA from ATII cells on plates not prepared for telomere measurement via HTQ-FISH, plates were centrifuged as above, supernatants were discarded, and cells were lysed by adding NZYol directly to the plates. 800 µl NZYol was used per sample.

To isolate RNA from ATII cells seeded in 96 well plates allowing for measurement of telomeres via HTQ-FISH, the supernatant was harvested in microcentrifuge tubes, centrifuged as above and the cell pellets were resuspended in 800 µl NZYol.

RNA isolation

Following resuspension in NZYol, the cell lysate was pipetted several times to homogenize, and samples were incubated for 5 minutes at room temperature. 0.18 ml of chloroform was added to each sample, tubes were capped and shaken vigorously for 15 seconds then incubated for 3 minutes at room temperature. Samples were centrifuged at 12,000 xg for 15 minutes at 4ºC and the upper aqueous phase was transferred to a new tube. RNA was precipitated by mixing 0.4 ml of cold isopropyl alcohol and incubated for 10 minutes at -20ºC. Samples were then centrifuged at 12,000 xg for 10 minutes at 4ºC and the supernatant was discarded with a micropipette. To wash the RNA, the pellet was resuspended in 0.8 ml of 75% ethanol. Samples were centrifuged at 12,000 xg for 5 minutes at 4ºC and the supernatant was again discarded. Samples were left to air dry for 15 minutes and the pellet was resuspended in 20 µl DEPC-treated water. The RNA concentration of samples was determined using a NanoDrop Spectrophotometer from NanoDrop Technologies and samples were stored at -80ºC.

Complimentary DNA (cDNA) Reverse transcription

Single-stranded cDNA was synthesized using the high-capacity cDNA reverse transcription kit from Applied Biosystems. 2 µg of RNA in a volume of 10 µl DEPC-treated water was loaded into a PCR tube. A 2X master mix containing 2 µl RT buffer, 0.8 µl dNTP mix, 2 µl RT random primers, 4.2 µl nuclease-free water and 1 µl MultiScribe reverse transcriptase per reaction was mixed on ice. 10 µl of master mix was added to each 10 µl RNA sample, mixed gently, sealed, and briefly centrifuged to spin down contents and eliminate air bubbles. A negative control containing 10 µl of master mix and 10 µl of DEPC-treated water was also prepared. Reactions were loaded to the thermal cycler. The thermal cycler was programmed according to the **Table 1** and the reaction volume was set to 20 µl.

Table 1: Program for thermal cycler for cDNA Reverse transcription.

Temperature (ºC)	Step 1	Step 2	Step 3	Step 4
	25	37	85	4
Time (minutes)	10	120	5	∞

SYBR Green Quantitative PCR (qPCR)

Table 2: Primers and probes used in qPCR.

Target gene/Probe	Forward(F)/Reverse(R)	Oligonucleotide sequence 5´to 3´
Human S14 (endogenous)	F	GGGGTGACATCCTCAATCC
	R	TATCACCGCCCTACACATCA
Human SPC	F	TGGTTACCACTGCCACCTTC
	R	CTGGCCCAGCTTAGACGTAG

A master mix for each target gene containing 5 µl SYBR green, 0.3 µl forward primer, 0.3 µl reverse primer and 3.4 µl Milli-Q water per reaction was mixed. The sequences of primers used can be seen in **Table 2**. 9 µl of master mix was pipetted into each well of a 0.2 ml PCR reaction plate from Applied biosystems. 1 µl of cDNA was loaded to each well. cDNA samples were then amplified by qPCR in triplicate reactions for each primer pair assayed on a 7500 Real-Time PCR Instrument (Applied Biosystems) using SYBR Premix Ex Taq (Takara Bio) and the following qPCR conditions: 95°C for 2 min; 40 cycles of 95°C for 15 s, 60°C for 15 s and 72°C for 60 s. Results were normalized using S14 rRNA gene as the endogenous control. Two negative controls containing 9 µl master mix and either 1 µl water or 1 µl of negative control from retro transcription were also performed for each target gene. Thresholds for gene expression were adjusted on the StepOne software and data was exported and analysed in Microsoft Excel. We applied the delta-delta Ct method (2-ΔΔct): ΔΔCt= ΔCt (SPC) – ΔCt (S14).

Conditions that allow measurement of telomere length via HTQ-FISH techniques in ATII cells

High-throughput telomere length quantification by FISH allows the quantification of telomere length through fluorescence, as well as showing the percentage of short telomeres in human cells, enabling the uncovery of associations between telomere length and human disease (*28*). The technique is aggressive and requires treatment at 80ºC so many cells can become detached in the process. Measuring of telomeres was carried out by Maria Blasco´s laboratory in CNIO, Madrid who are collaborating in this project, so plates also needed be sealed with adhesive plate seals from Thermo Scientific and to withstand shipping. Black, clear bottomed microplates from Greiner bio-one were used and depending on the type of cells being measured, plate coatings may be required. Cells need to be numerous enough, but not too numerous to allow measurement and so the number of cells required varies depending on the size of cells, how well they attach to the plate and how many are lost during fixing and measurement processes. As the collaborating laboratory had never measured telomeres of ATII cells before, it was necessary to find the conditions needed for the technique.

In order to measure SPC gene expression and telomere length in parallel under the same cell culture conditions, cells were seeded and treated and 24 hours later the supernatant was harvested for RNA extraction and measuring gene expression, and remaining cells attached to the plate, were fixed to enable telomere measurement.

To establish the number of cells and the optimal coating required to allow measurement of telomere length via HTQ-FISH techniques in ATII cells, a 96 well plate was prepared with 3 different coatings, and controls without coating, and seeded with 100,000 200,000, 300,000 and 400,000 cells per well.

96-well plate coatings

Poly-L-Lysine solution 0.1% from Sigma was diluted 1:1 with Milli-Q water and 100 µl was plated per well.

1.02 mg of Gelatin from porcine skin by Sigma was dissolved in 3.2 ml Milli-Q water, filtered through a 0.2 µm filter from Minisart, and 100 µl was plated per well.

0.31 ml of Matrigel matrix from Corning was mixed with 5.69 ml DMEM on ice, and 100 µl was plated per well.

The plate was incubated with coatings at 37ºC for 2 hours, coatings were then discarded, wells were rinsed with DMEM before cells were seeded.

Plate fixation for HTQ-FISH

Supernatants were removed after 24 hours of incubation for RNA extraction, as outlined above, and cells attached to the plate were gently rinsed with 100 µl PBS and fixed by adding 200 µl of fixation solution containing methanol: acidic acid 3:1 to each well, incubating for 5 minutes then discarding the fixation solution. This process was repeated 3 times in total leaving the fixation solution for 45 minutes the final time and freezing at -80ºC. The plate was sealed and sent to Madrid for measurement of telomere length via HTQ-FISH.

SARS-CoV2 infection of ATII cells

Directly following extraction, ATII cells were seeded 100,000 cells in 100 µl cell culture medium per well on a 96 well plate coated with Matrigel as outlined previously. Cells were taken into the Biological Containment Laboratory (BSL-3 laboratory) in the IBBTEC and were infected with SARS-CoV-2. Researchers accredited to work in NCB3 security laboratories performed these experiments and inactivated the virus by hydrogen peroxide before removing the samples from the BSL-3 laboratory. A serial dilution of the virus was performed, and cells were infected with the following:

0 ul: 0 titres de virus (plaque forming unit (PFU)) MOI= 0

25 ul: 6.1x104 titres of virus PFU. MOI= 1.25

14 ul: 5x105 titres of virus PFU. MOI= 0.7

7 ul: 3.2x104 titres of virus PFU. MOI= 0.35

3.5 ul: 1.7x104 titres of virus PFU. MOI= 0.175

1.8 ul: 8.8x103 titres of virus PFU. MOI= 0.09

0.9 ul: 4.5x103 titres of virus PFU. MOI= 0.045

0.5 ul: 2.5x103 titres of virus PFU. MOI= 0.025

3 replicas of each concentration were performed as well as 6 replicas of non-infected control wells. Following 24 hours of infection, supernatants were removed, 3 replica wells were combined in microcentrifuge tubes and RNA extraction and reverse transcriptase were performed as detailed above to enable gene expression analysis. The plate was rinsed with PBS and fixed to be sent for HTQ-FISH

analysis as outlined above. The virus was inactivated by hydrogen peroxide and RNA extraction was performed as outlined above. SYBR green qPCR was performed to enable gene expression analysis of SPC and S14, and CDC 2019-nCoV real-time RT-PCR diagnostic panel was preformed to detect virally produced RNA and confirm SARS-CoV-2 infection of cells.

CDC 2019-nCoV real-time RT-PCR diagnostic panel

Table 3: Primers and probes used in 2019-nCoV real-time RT-PCR.

Target gene/Probe	Primer description
Human Ribonuclease P (RP) (extraction control)	Human RNase P Forward Primer/Probe mix
Nucleoprotein gene (N1)	2019-nCoV_N1 Combined Primer/Probe mix
Nucleoprotein gene (N2)	2019-nCoV_N2 Combined Primer/Probe mix

Master mixes were mixed for each target gene RP, N1 and N2 containing 5 µl TaqPath 1-step RT-qPCR master mix, 1.5 µl of combined primer/probe mix and 8.5 µl nuclease-free water per number of reactions. 15 µl of each master mix was dispensed into the appropriate wells and 5 µl of sample was added to each well. Negative controls for each target gene contained 5 µl nuclease-free water. Plates were run on Applied Biosystems Real-time PCR instrument. StepOne software from Thermo Fisher Scientific was used to run the standard curve (absolute quantification) PCR. Stage 1, 2 minutes at 25ºC; 1 repeat. Stage 2, 15 minutes at 50ºC; 1 repeat. Stage 3, 2 minutes at 95ºC; 1 repeat. Stage 4, 3 seconds at 95ºC, 30 seconds at 55ºC; 45 repeats. Thresholds for gene expression were adjusted on the StepOne software and data was exported and analysed in Microsoft Excel.

Cell culture conditions to test the effect of plant extracts on SPC expression in ATII cells

Directly following extraction, ATII cells from two different patients were seeded 100,000 cells in 100 µl cell culture medium per well on 96 well plates coated with Matrigel as outlined previously. 4 total metabolite (TM) plant extracts from *Marchantia* and 4 total metabolite plants extracts from *Arabidopsis* were suspended in the required volume of DMSO to give a final concentration of 0.4 mg/ml when 2 µl was added to wells. Plant extracts were provided by the Institute of Biomedical Research of Barcelona (IIBB-CSIC) who are collaborating in this project. Plant extracts were suspended in DMSO due to their high liposolubility but because DMSO can be toxic to cells, 2 µl of DMSO was added to control conditions. Following the addition of plant extracts, TGF-β was added to give either a final concentration of 3 ng/ml or 1 ng/ml. Experiments performed in this laboratory by other students showed that TGF-β concentrations of 3 ng/ml and 1 ng/ml activated collagen expression in fibroblasts. Control

conditions contained TGF-β 0 ng/ml, 1 ng/ml, or 3 ng/ml with 2 µl DMSO and no plant extracts. 6 replicates of each condition were performed. Cells were harvested and pooled from 3 wells for gene expression analysis as detailed previously, providing 2 biological replicas of each condition. Cells attached to plates were fixed for HTQ-FISH analysis.

The plant extracts used in this experiment (TM1-TM8) were all total metabolites from mutant expressor lines of *Marchantia polymorpha* and *Arabidopsis thaliana* and can be seen in **Table 4**.

Table 4: Plant extracts from *Marchantia p* and *Arabidopsis t.*

Name	Mutant	Plant species	Colour of pellet
TM1	Mp_Tak1	*Marchantia p*	beige
TM2	Mp_Tak2	*Marchantia p*	beige
TM3	Mp_CYP85mut	*Marchantia p*	beige/orange
TM4	Mp_Det2mut	*Marchantia p*	beige/orange
TM5	At_Col-0 mock	*Arabidopsis t*	light brown
TM6	At_Col-0 sorbitol	*Marchantia p*	brown
TM7	At_BRL3ox	*Arabidopsis t*	red
TM8	At_DWARFox	*Arabidopsis t*	light brown

Isolation of human fibroblasts from clinical lung samples

Samples were cut into 1 mm^3 explants and placed on 6 well plates with 10 explants per well in a safety cabinet. They were allowed to attach for 10 minutes before gently adding 3 ml of the above-mentioned cell culture medium being careful not to detach explants. Plates were incubated at 37°C in 5% CO_2. The medium was replaced every 4 days. After approximately 3 weeks, fibroblasts were visible in the microscope. Once 80% confluence was reached, explants were removed, and cells were rinsed with 1 ml PBS and cell medium was replaced. The first sub-culture was performed by removing culture medium, washing with 1 ml PBS, adding 1 ml 1x trypsin-EDTA to each well and incubating at 37°C for 3 minutes. To stop trypsinization, 1ml of culture medium supplemented with 10% FBS was added, and cells were centrifuged at 400 xg for 5 minutes at room temperature. The supernatant was discarded, the pellet resuspended in culture medium and the cells seeded in a 60 × 15 mm tissue culture dish. Once 3 passes had been performed, cells were frozen in culture medium containing 10% Dimethyl sulfoxide (DMSO). Fibroblasts were defrosted by adding 1 ml warm cell culture medium to the vial of frozen cells and gently pipetting up and down until the cells were defrosted. Cells were centrifuged for 3 minutes at 400 xg and resuspended in cell culture medium.

Results

Detection of human ATII cells isolated from clinical lung samples

ATII cells were successfully isolated from the lung samples of 26 patients. Histochemical staining with alkaline phosphatase showed the purity of ATII cells varied between patients from 21% to 51%. **Figure 1** shows some examples of the areas of the scanned slides containing 250,000 cells and used to calculate the percentage of ATII cells present (pink/purple-coloured cells). It also highlights the variation in terms of cells appearance, number of cells per area and contaminants among patients.

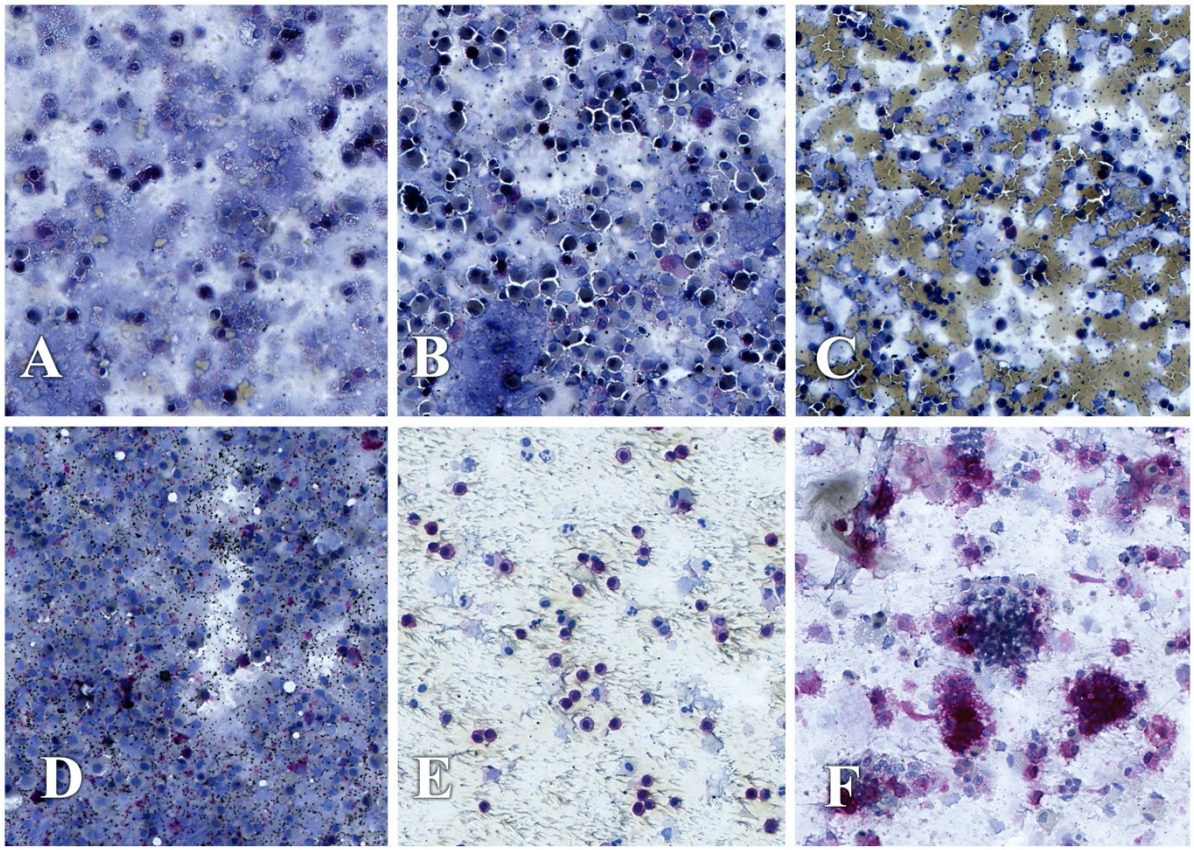

Figure 1: Examples of selected areas of alkaline phosphatase histochemical staining of human ATII cells (in purple) from clinical lung samples. A, B, C, D, E and F are images from patients 4, 13, 20, 21, 23 and 24 respectively.

The mean values and standard deviation values of the percentage of ATII cells per purification process is 36.3±10.8, with n=10. **Table 5** shows the percentage of ATII cells calculated in the patient samples which were measured. Samples from patients 4 to 21 were cytocentrifuged after cells had been frozen and defrosted whereas samples from patients 23 to 27 were cytocentrifuged directly after extraction. Frozen and defrosted cells did not show a significantly lower percentage (Student T test) of ATII cells (29,8 ± 4,6; N=4) compared to fresh cells (41,6 ± 4,3; N=5) as can be seen in **Figure 2**. This result

shows a tendency of obtaining higher percentage of AT II cells in fresh cells, indicating the possibility of loss of ATII cells in the freezing and thawing process. A larger number of samples per group should be analysed to define if this tendency could become a significant difference in the percentage of ATII cells in fresh cells.

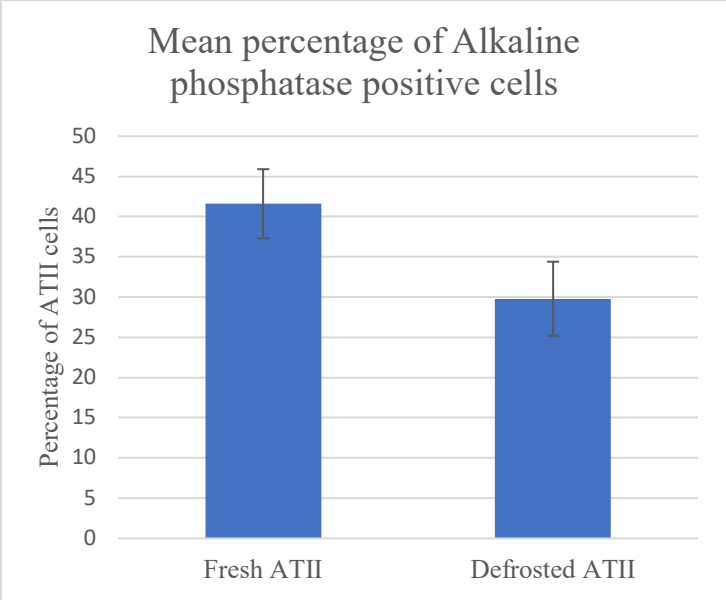

Figure 2: Mean percentage of Alkaline phosphatase positive cells from cells that were fresh, and cells that had been frozen and defrosted, after ATII cell extraction

Table 5 shows the percentage of ATII cells calculated in the patient samples which were measured. Samples from patients 4 to 21 were cytocentrifuged after cells had been frozen and defrosted whereas samples from patients 23 to 27 were cytocentrifuged directly after extraction.

Table 5: Percentage of Alkaline phosphatase positive cells in ATII cell extractions

Patient number	Alkaline phosphatase positive cells
4	42%
13	25%
20	21%
21	31%
23	51%
24	40%
25	27%
26	40%
27	50%

ATII cell viability over a 24-hour period

To Establish cell viability over a 24-hour period, cells from patient 5 were defrosted, counted, and seeded as outlined above. 6 replicas were performed. **Figure 3** shows the percentages of alive and dead cells counted at each 12-hour interval. After 12 hours, viability is seen to decreased but after 24 hours there is no significant change in viability compared to 0 hours. At 0 hours the mean average percentage of alive cells was 59.1%, this decreased to 50.6% after 12 hours and increased again to 59.0% after 24 hours. Percentage of ATII cells alive at 0 hours and after 24 hours did not show a significant difference (Student T test) between 0 hours (59.1 ± 1.9; N=6) compared to 24 hours (59.0 ± 1.8; N=6).

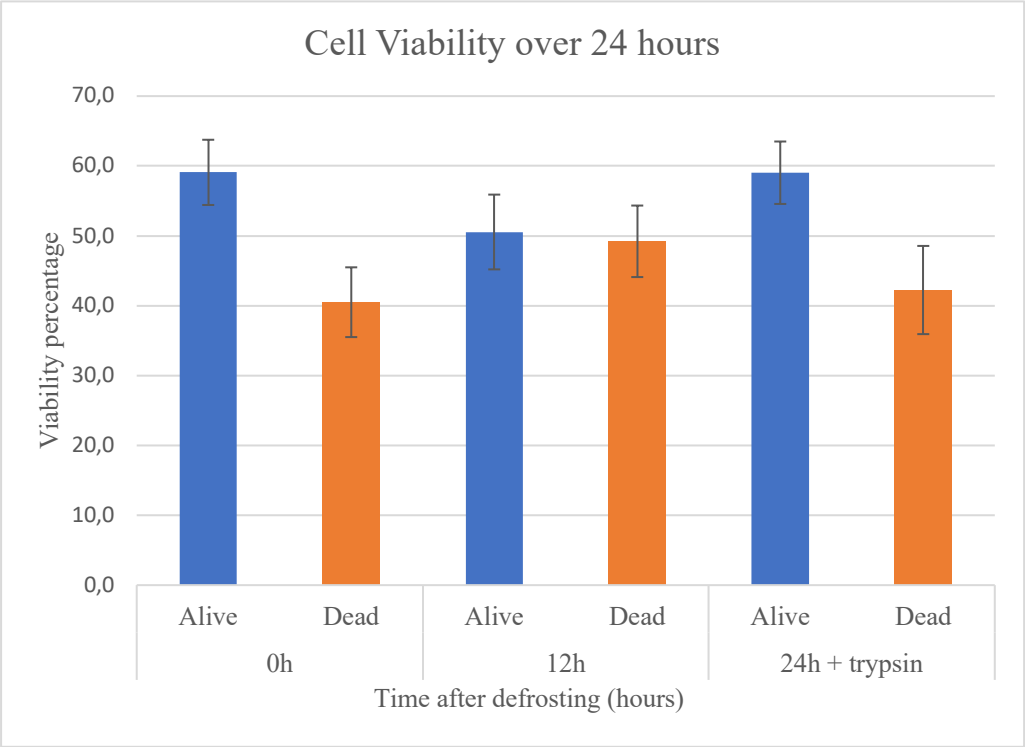

Figure 3: The mean average of alive and dead cells from patient 5 over a period of 24 hours. Averages were calculated from 6 replica wells and cells were stained with Trypan Blue and counted using a haemocytometer.

SPC expression in ATII cells 0h, 24h and 48h after defrosting

Initial experiments used 50,000 defrosted ATII cells from patient 5. We do not have an alkaline phosphatase analysis for patient 5 but using the mean percentage of ATII cells per sample (29,8%) we can assume that approximately 15,000 were ATII cells. No gene expression of either the endogenous gene S14 or SPC gene was obtained.

The number of cells seeded was increased and RNA was extracted at 3 time-intervals; immediately after being defrosted at 0 hours (0h), after 12 hours (12h) and 24 hours (24h). Cells from patient 5 were

defrosted and counted. 2 replicates of 120,000 cells each were prepared for RNA extraction immediately after being defrosted. According to the mean percentage of ATII cells per sample, approximately 35,000 of these cells would have been ATII cells. Remaining cells were plated 100,000 cells (30,000 of which would have been ATII) per well in 400 µl of cell culture medium on a 24 well plate. 24 hours later, the supernatants of 2 replica wells were harvested, and after 48 hours, cells from the remaining 2 wells were harvested for RNA extraction.

The relative SPC gene expression from defrosted cells (120,000 cells) offered quite a high variability between replicas but both were higher that 24 and 48 hours. The relative SPC gene expression from cells defrosted and plated for 24 hours (100,000 cells) reduced at least 0,5 arbitrary units in the first 24 hours following defrosting. The relative SPC gene expression from cells defrosted and plated for 48 hours (100,000 cells) didn´t reduce significantly more compared to 24 hours. The reduced number of replicas performed did not allow us to provide statistical differences (n=2 named as "a" and "b" in **Figure 4**) but showed preliminary changes in SPC expression over 48 hours of ATII cell culture.

Figure 4 shows the change in SPC expression over a 48-hour period in ATII cells. There was also quite a high variability in the expression between the 0h replicas.

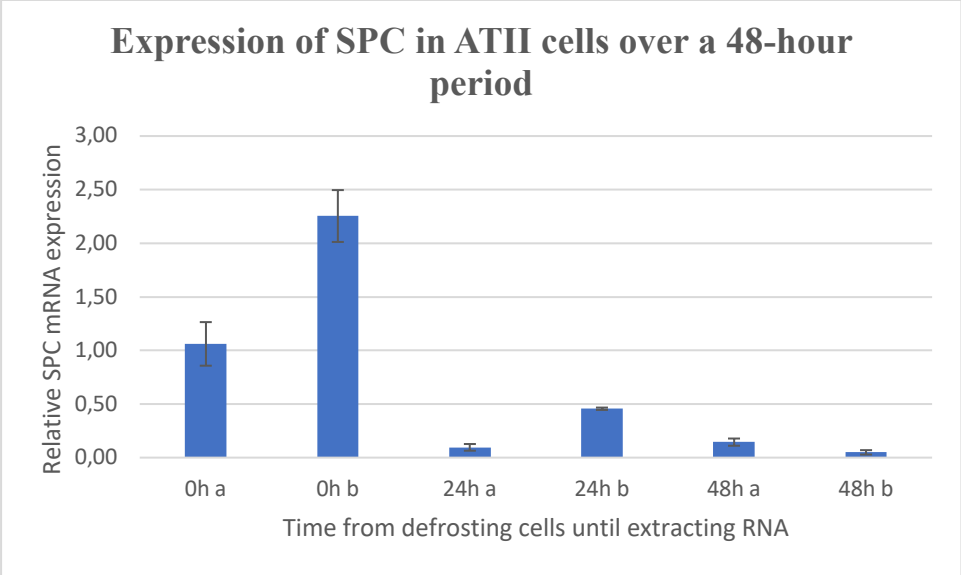

Figure 4: Relative expression of SPC in ATII cells from patient 5 over a 48-hour period. 0h, 24h and 48h refer to the number of hours from the time of defrosting cells to the time of extracting RNA and a and b refer to biological replicas. Each biological replica has its own technical triplicate

Effect of TGF-β in ATII cells on SPC expression

TGF-β was chosen to imitate the effects of a cytokine storm in cells because of both the high levels of TGF-β in COVID-19 patients and for its role in activating fibroblasts and initiating fibrosis (*29*). We

did not detect any reduction in SPC gene expression due to the three different concentrations of TGF-β (0 ng/ml, 1 ng/ml, or 3 ng/ml) in ATII cells. 2 replicas (named a and b) were performed for each condition (0 ng/ml, 1ng/ml, and 3ng/ml of TGF-β). To obtain these results, 150,000 cells in 100 µl cell culture medium from patient 22 were seeded in 6 wells of a 96 well plate immediately following cell extraction. TGF-β stock of 60 ng/ml was diluted in phosphate-buffered saline (PBS) and used to treat cells giving a final TGF-β concentration of 1ng/ml or 3ng/ml. An equal quantity of PBS was added to the TGF-β 0 ng/ml control wells.

Figure 5 shows how SPC gene expression is not negatively affected when increasing concentrations of TGF-β are used to treat the cells compared to the control sample (no TGF-β). In the graph, a and b refer to biological replicas. The general trend shows that SPC expression increased with the addition of TGF-β. However, there are differences of 2-3 arbitrary units between biological replicas, and differences of less than 2 arbitrary units in technical replicas in most cases.

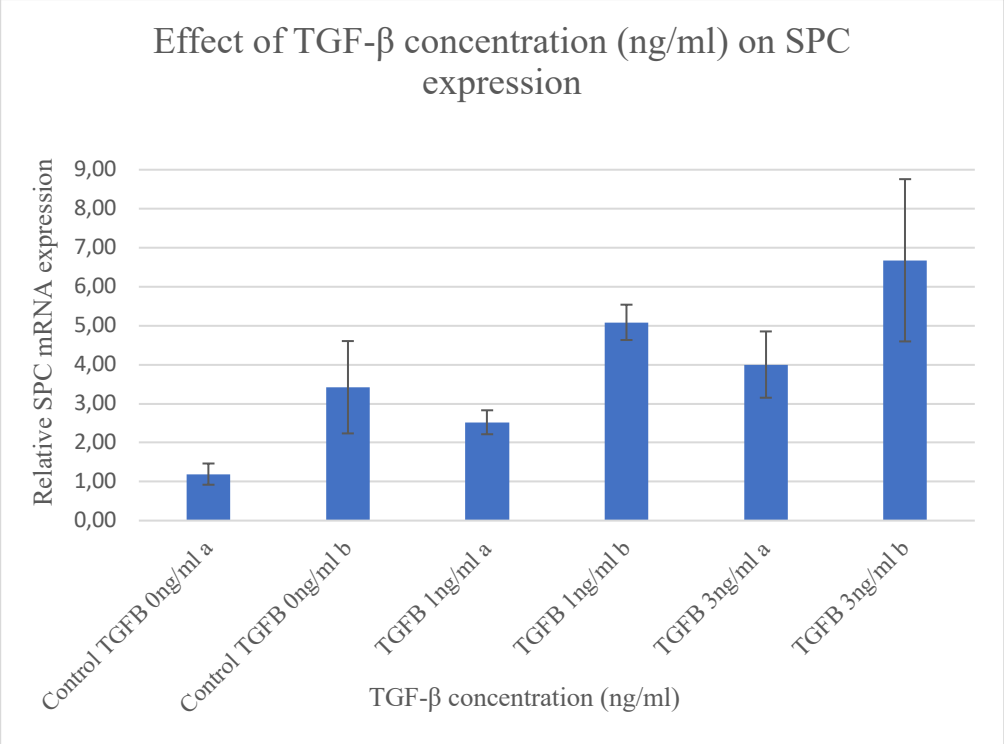

Figure 5: Effect of TGF-β on SPC gene expression in ATII cells from patient 22. A and b refer to biological replicas. Each biological replica has its own technical triplicate.

Conditions that allow measurement of telomere length via HTQ-FISH techniques in ATII cells

Both the number of cells and the optimal coating required to allow measurement of telomere length via HTQ-FISH techniques in ATII cells needed to be established. Initially a 96 well plate coated with poly-l-lysine containing 20,000 to 60,000 cells per well was seeded and fixed 24 hours later. The initial

60,000 cells proved that at the end of the hybridization process with appropriate primers and probes including aggressive temperature conditions (80°C) the number of cells was reduced and was insufficient for the analysis of the mean telomere length of the sample. However, telomeres could be visualised as red spots, from a specific red fluorophore complementary to DNA-telomere sequence, within dapi-stained nuclei in the tested wells as can be seen in **Figure 6**.

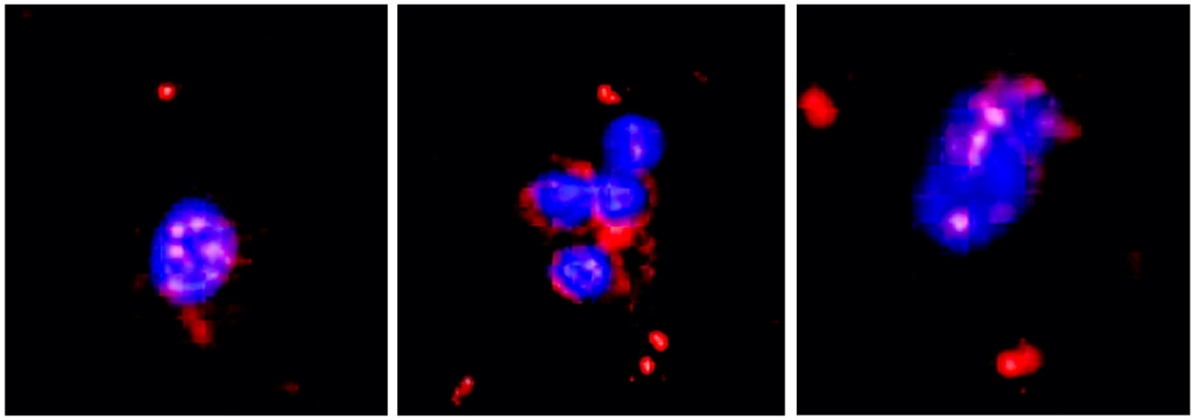

Figure 6: Representative fluorescent images of telomeres (red) and nuclei (blue) obtained with HTQ-FISH technique containing initial 60,000 cells per well. The number of cells remaining on the plate was insufficient for determining telomere length.

To establish the number of cells and the optimal coating required to allow measurement of telomere length via HTQ-FISH techniques in ATII cells, another 96 well plate was prepared with 3 different coatings, and controls without coating, and seeded with 100,000 200,000, 400,000 cells per well from patient 23. 100,000 200,000, 400,000 total cells correspond to 50,000, 100,000 and 200,000 AT II cells following Alkaline phosphate analysis according to **Table 5**.

Wells containing 300,000 total cells (corresponding to 120,000 AT II cells according to **Table 5**) from patient 24 were seeded directly following cell purification.

We proved that we could obtain SPC gene expression in plates that are subsequently sent to CNIO for telomere length measurement (**Figure 7**). By combining both techniques with the same sample we ensure that we have the methodology ready to test whether differences in telomere length correspond to variations in SPC expression within the same sample.

We observed that in the case of 200,000 total cells, changing the coating did not reduced SPC expression by more than the difference between control replicas a and b however Matrigel increased SPC expression by over 2 arbitrary units. In the case of 400,000 total cells, SPC expression levels were similar in control, Gelatin and Matrigel though expression of SPC on poly-l-lysine was reduced by almost 2 arbitrary units compared to control cells. In the case of 600,000 cells, gelatine shows similar levels of SPC expression to control cells, expression of SPC in cells on poly-l-lysine is very low and on Matrigel is increased compared to control cells. In the case of 800,000 cells, expression of SPC is similar

to that of 600,000 cells with very low expression in cells on poly-l-lysine and Gelatin however expression in control cells is slightly higher than cells on Matrigel. Results can be seen in **Figure 7.**

To obtain these results, all cells were seeded in 100 µl cell culture medium and incubated at 37ºC. After 24 hours of incubation, supernatants were carefully removed and transferred to microcentrifuge tubes pooling the contents of two duplicate wells, and RNA was extracted as outlined above to enable analysis of SPC expression. Cells remaining on the plate were fixed and sent to CNIO for telomere length measurement.

Cells plated on Matrigel consistently demonstrated expression of SPC equal to or higher than those of control cells so except in the case of 800,000 cells where expression was just below that of the control cells but still higher than that of poly-l-lysine or Gelatin. For this reason, Matrigel was selected for future experiments.

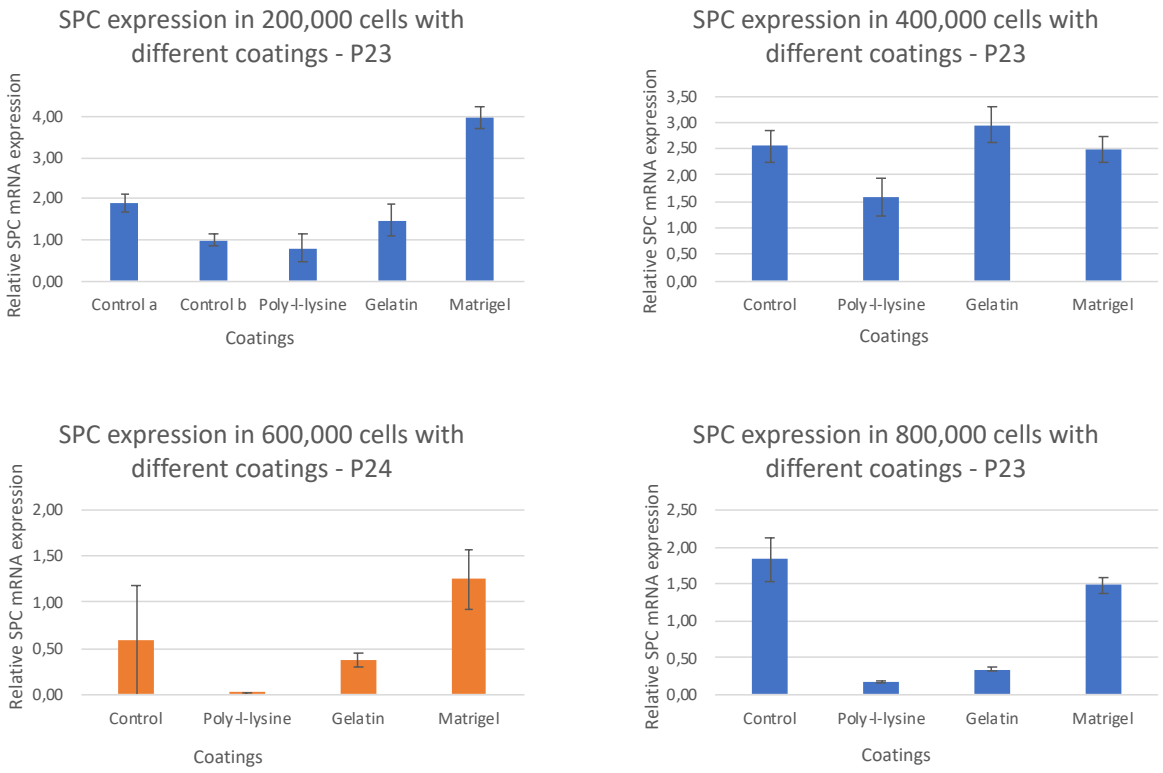

Figure 7: Relative expression of SPC with a varying number of cells and different plate coatings compared to controls without any coating. P23 and P24 refer to patient 23 and 24 and are highlighted in blue and orange respectively. Control a and b are biological replicas. Statistical differences cannot be obtained because n=2 (a and b). Each biological replica has its own technical triplicate.

Figure 8 shows how SPC expression varies according to number of ATII cells pooled for each RNA extraction. Regardless of coating used, 200,000 cells were sufficient to have expression of SPC. In all conditions except cells plated on Matrigel, 400,000 cells gave the highest expression of SPC, on

Matrigel control cells gave a higher expression of SPC. In all conditions 600,000 cells from patient 24 gave the lowest expression of SPC compared to other number of cells from patient 23. 800,000 cells showed a reduced expression of SPC under all conditions except control cells where SPC expression in 800,000 cells was similar to that of 200,000 cells. The Matrigel coating is selected for following assays shown in this study because the SPC gene expression values obtained were the highest (from 1-4 arbitrary units) compared to the other coatings tested (from 0-3 arbitrary units) in all conditions tested. Telomere length has not yet been measured in these samples via HTQ-FISH.

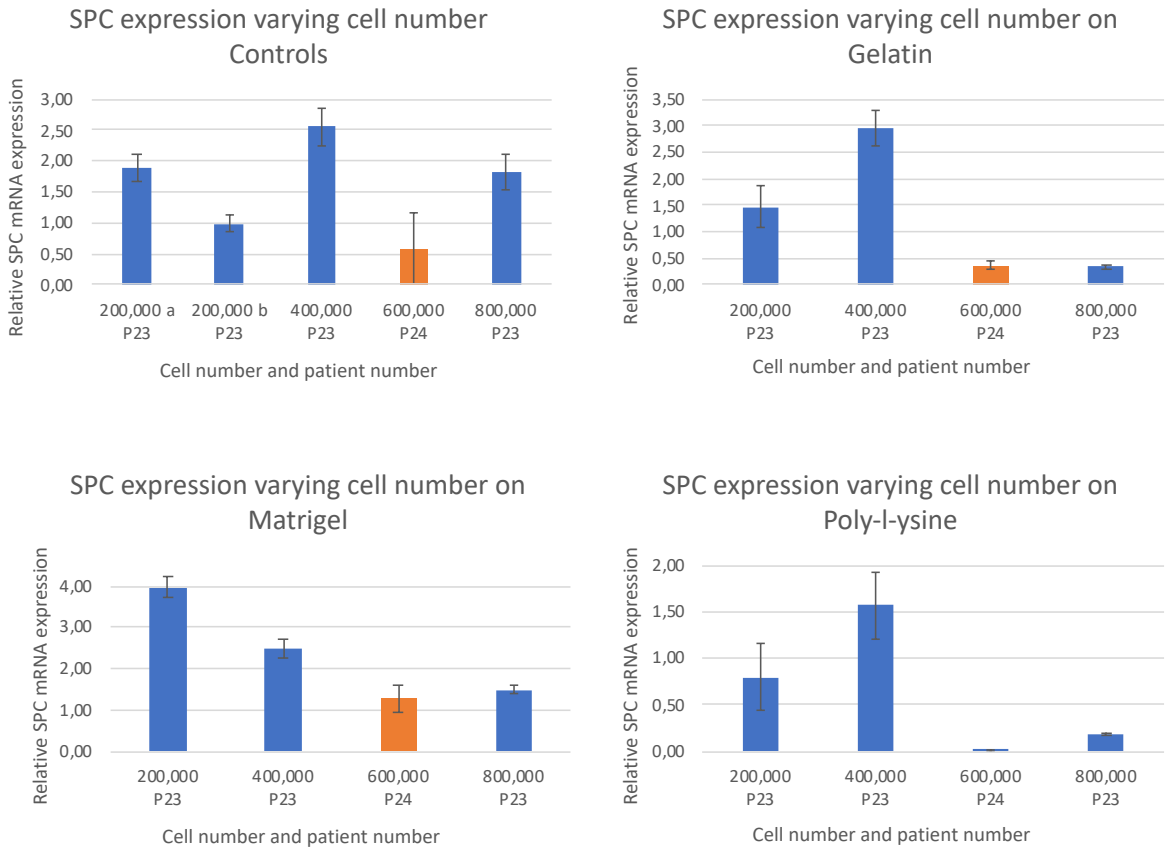

Figure 8: SPC expression according to number of ATII cells pooled for RNA extraction seeded on different coatings. P23 and P24 refer to patient 23 and 24 and are highlighted in blue and orange respectively. Control a and b are biological replicas. Each biological replica has its own technical triplicate.

CDC 2019-nCoV real-time RT-PCR diagnostic panel

Directly following extraction, ATII cells from patients 27 and 28 were seeded 100,000 cells in 100 µl cell culture medium per well on a 96 well plate coated with Matrigel. According to **Table 5,** 50,000 ATII cells of patient 27 were seeded in each well and we do not have alkaline phosphatase analysis for patient 28. Cells were infected with SARS-CoV-2 with 0 ul, 25 ul, 14 ul, 7 ul, 3.5 ul, 1.8 ul, 0.9 ul and 0.5 ul titres of virus as outlined in the methods section. 3 replicas of each concentration were performed

as well as 6 replicas of non-infected control wells in each patient. Cells from 3 replicas were pooled for RNA extraction to increase the number of cells per assay for SPC gene expression assays. Plates were fixed for telomere measurement as outlined above and RNA was extracted and retrotranscribed and used for both CDC 2019-nCoV real-time RT-PCR diagnostic panel to confirm SARS-CoV-2 infection and to measure SPC gene expression.

The results of CDC 2019-nCoV real-time RT-PCR diagnostic panel are valid when cycle threshold (CT) values for RP are below 40, and cells are infected with SARS-CoV-2 when either N1, N2 or both have CT values under 40. **Table 6** shows all results for patient 27 were valid and all cells infected with a viral titre above 0 were successfully infected. Negative controls were not infected. The general trend showed that N1 and N2 CT values inversely correlated with viral titre.

Table 6: CDC 2019-nCoV real-time RT-PCR diagnostic panel of ATII cells from patient 27. CT is cycle threshold, Std Dev is the standard deviation between triplicates of the PCR. Viral titre units (ul). Undetermined results mean values were too low to be detected by the equipment

Viral titre (ul)	RP Cт Mean	RP Std Dev	N1 Cт Mean	N1 Std Dev	N2 Cт Mean	N2 Std Dev
0 (a)	31,47	0,20	Undetermined	Undetermined	Undetermined	Undetermined
0 (b)	36,81	1,38	Undetermined	Undetermined	Undetermined	Undetermined
0.5	37,63	0,01	34,26	0,17	37,48	0,31
0.9	37,64	0,05	36,03	0,65	39,87	Undetermined
1.8	36,72	0,34	30,59	0,24	33,88	0,16
3.5	38,03	0,57	31,75	0,29	34,57	0,20
7	32,68	0,09	25,89	0,06	31,06	0,77
14	38,21	Undetermined	32,21	0,27	34,55	1,35
25	30,58	0,08	24,19	0,16	26,55	0,10

SPC expression in SARS-CoV-2 infected ATII cells

Results from the qPCRs in patient 28 showed that SPC expression was low in controls, higher SPC expression was seen in viral titres of 7 ul and 3.5 ul however standard deviation was also high in these samples, and no SPC expression was seen under all other conditions. CT numbers were all above 32 and many wells were undetermined. In Patient 27, SPC expression was seen in both controls, high SPC expression was seen in 25 titres of virus, no SPC expression was seen in viral titres of 14 and 7 and 0.9 and very low expression was seen in viral titres of 3.5 ul, 1.8 ul, and 0.5 ul. There were also many wells with an undetermined CT value. The only viral titre to show SPC gene expression in both patients was 3.5 ul. Results can be seen in **Figure 9**.

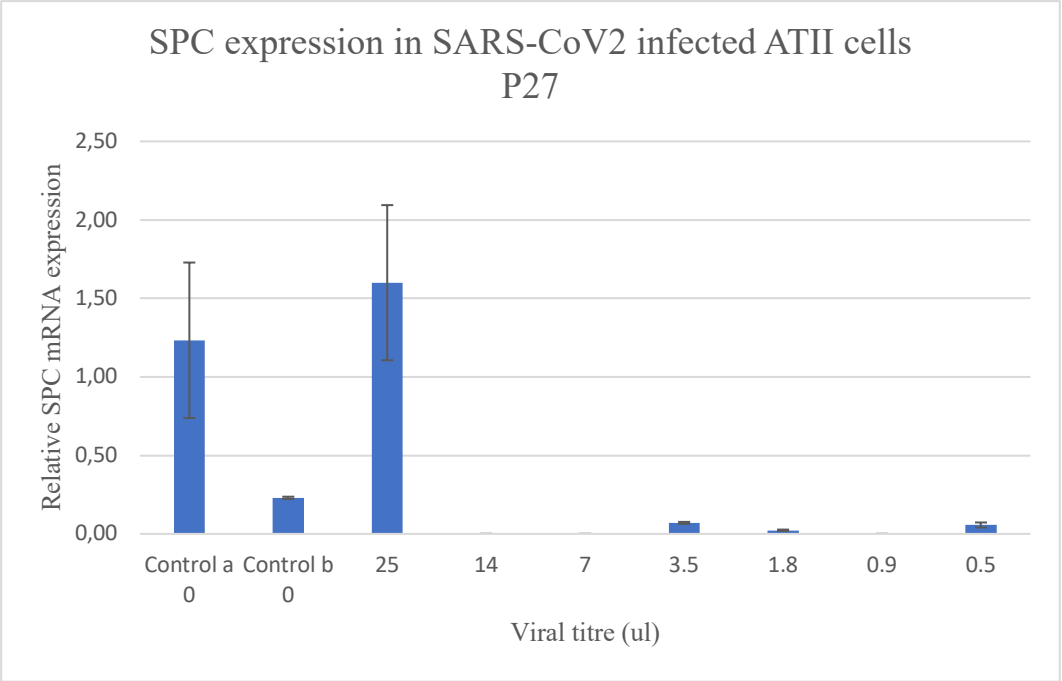

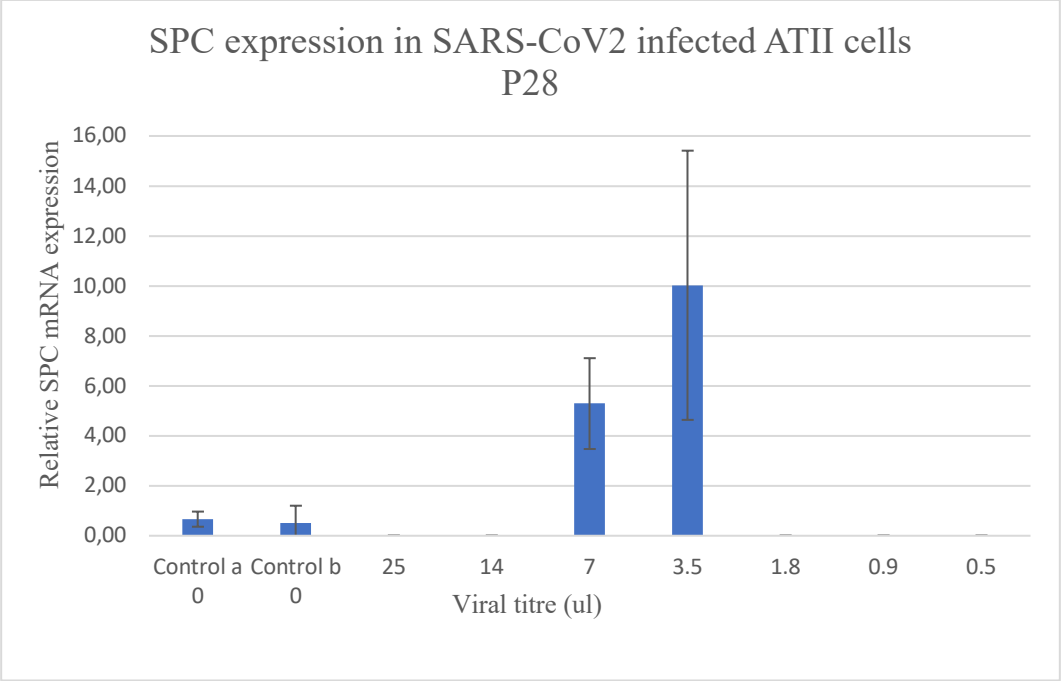

Figure 9: SPC expression in SARS-CoV-2 infected ATII cells of patient 27 and 28. Controls were not infected with the virus and a and b refer to biological replicas. Each biological replica has its own technical triplicate.

SPC expression in plant extract treated ATII cells

Directly following extraction, ATII cells from patients 25 and 26 were seeded 100,000 cells in 100 µl cell culture medium per well on 96 well plates coated with Matrigel as outlined previously. According to **Table 5**, 100,000 total cells would be 27,000 ATII cells per well for patient 25 and 40,000 ATII cells for patient 26. Total metabolites from 4 plant extracts from *Marchantia* and total metabolites from 4

plants extracts from *Arabidopsis* were screened (**Table 4)**. Plant extracts were suspended in DMSO to give a final concentration of 0.4 mg/ml when 2 µl was added to wells. 2 µl of DMSO was added to control conditions. Following the addition of plant extracts, TGF-β was added to give either a final concentration of 3 ng/ml or 1 ng/ml. Control conditions contained TGF-β 0 ng/ml, 1 ng/ml, or 3 ng/ml with 2 µl DMSO and no plant extracts. 6 replicates of each condition were performed. Cells were harvested by pooling 3 wells for gene expression analysis as detailed previously, providing 2 biological replicates of each condition. Cells attached to plates were fixed for HTQ-FISH analysis.

Figure 10 Shows SPC gene expression in ATII cells in the presence of plant extracts M1-M8 of two biological replicas of patient 25 (**Figure 10 A** and **Figure 10 B**) and one replica in patient 26 (**Figure 10 C**) all from plates where 3 ng/ml TGF-β was added to all wells except controls. Results from other conditions (patient 26 replica a, and plates with TGF-β 1ng/ml) are still pending. **Figure 10 A** shows that expression of SPC does not appear to be altered significantly by the addition of plant extracts except in the cases of plant extract M3 where cycle threshold was undetermined in both S14 and SPC, and in the case of M4 where expression of SPC was higher compared to control cells. **Figure 10 B** shows SPC expression in TGF-β 3ng/ml is higher than the control and wells containing plant extracts. In biological replicas b, SPC expression with TM3 is observed and SPC expression in the presence of TM4 is reduced contrary to replicas a. Figure 10 C shows no SPC expression in presence of TM2 and highest SPC expression in the presence of TM7, unlike Figure 10 B where SPC expression in the presence of TM7 was the lowest of all conditions. Overall, SPC expression between all conditions does not vary more than 2.5 arbitrary units.

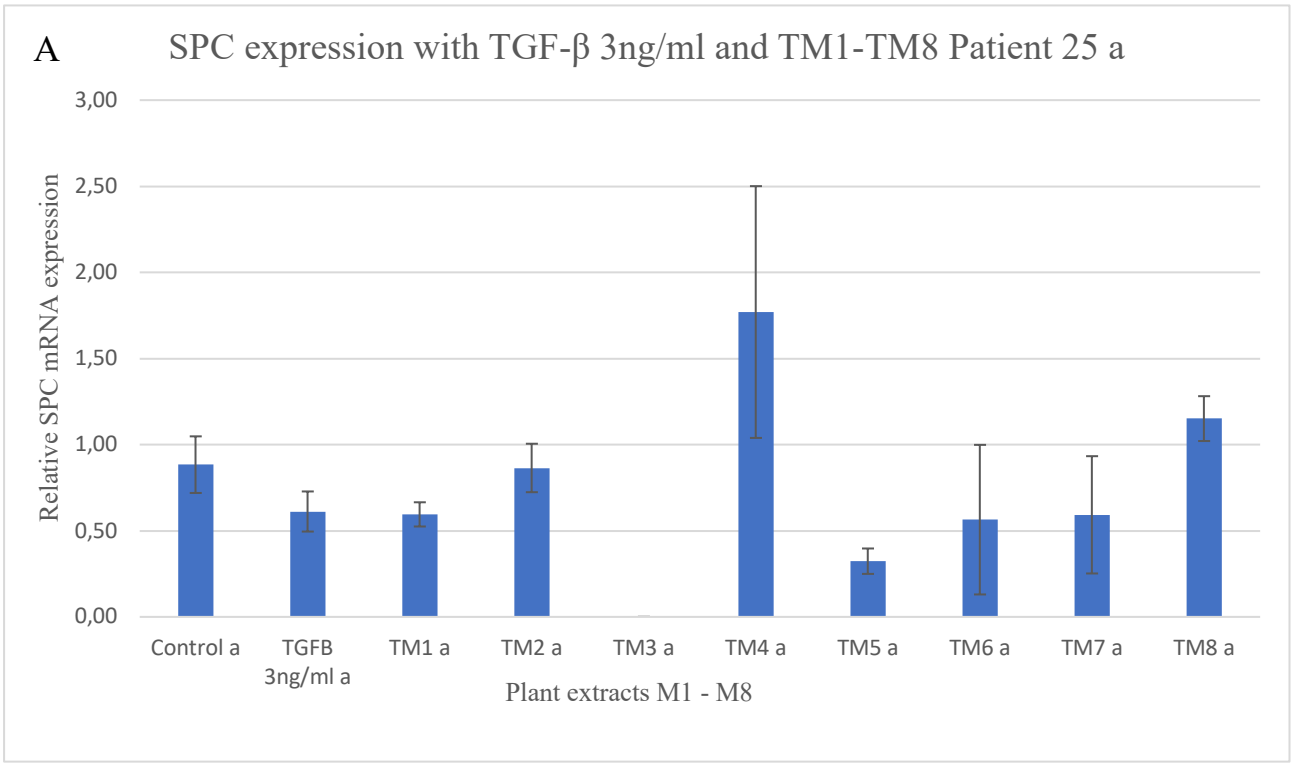

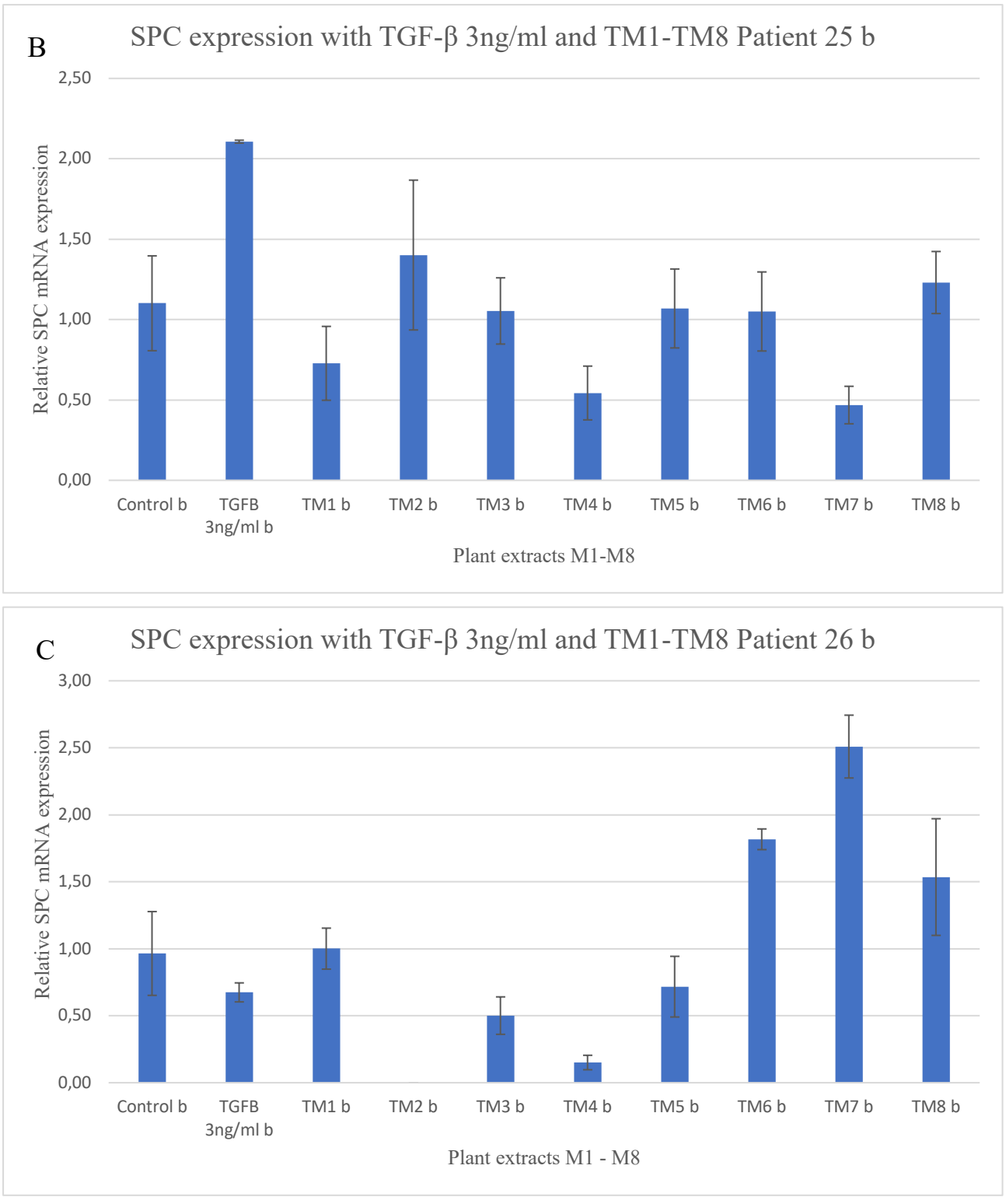

Figure 10: A) SPC gene expression in ATII cells from patient 25 replicas (a), treated with plant extracts 1-8 (M1-M8). B) SPC gene expression in biological replicas (b) of patient 25. C) SPC gene expression of ATII cells from patient 26 replica (b). All wells were treated with 3 ng/ml TGF-β except for control cells. Each biological replica has its own technical triplicate.

Cell culture of human fibroblasts from clinical lung samples

Human fibroblasts were successfully isolated from 3 patient´s lung samples. It took approximately 2 weeks for fibroblasts to become visible in the microscope. An image of the cells can be seen in **Figure 11**. Cells were identified morphologically. Over 200 million fibroblasts were frozen for future experiments.

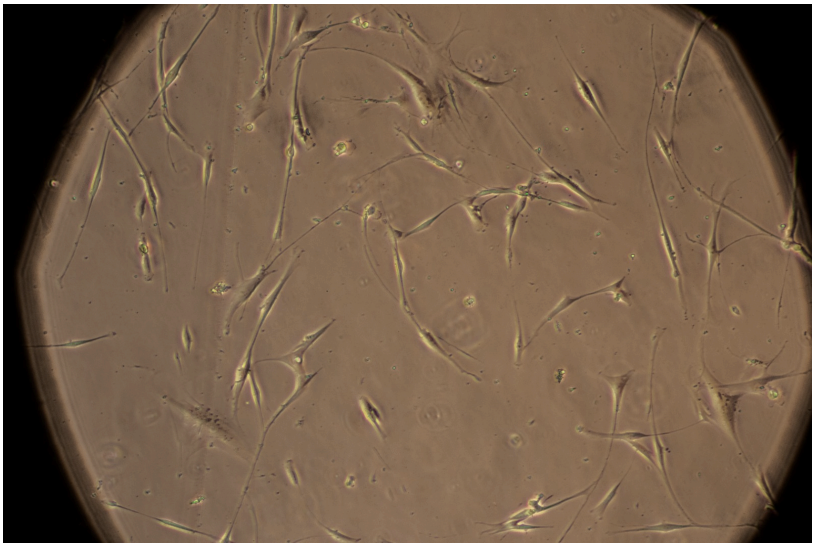

Figure 11: Representative bright field photo of pulmonary fibroblasts from patient 3

Discussion

In this study, we analysed the purity of ATII cells when extracted from human lungs, the maintenance of ATII homeostasis under different cell culture conditions, TGF-β treatments and SARS-CoV-2 infection and looked for the preservation of ATII cell health by the addition of plant extracts. Moreover, ATII cells were prepared under the conditions required to allow measurement of their telomeres by HTQ-FISH techniques in collaboration with the CNIO.

In addition, successful purification and cell culture of human lung fibroblasts were achieved to enable further assays to test the generation and prevention of fibrosis.

Isolation and histochemical staining of human ATII cells from clinical lung samples

Histochemical staining of ATII cells highlights the variability of patients and the low percentage of ATII cells. Improvements should be made in some key purification steps, such as reducing the size of the cut lung pieces before filtering, or longer incubations to remove adherent cells.

The percentage of alkaline phosphatase positive ATII cells (especially from frozen cells) was very low, this could explain lack of, or low gene expression in some initial experiments. Some samples had a higher total concentration of cells on the microscope slide, potentially limiting the penetration of alkaline phosphatase therefore leading to an under-estimation of the actual percentage of ATII positive cells. Considerable variation was also seen between patients in the amount of blood cell contamination and other lung contaminants. Therefore, it is quite possible that, depending on the type of pathology that patients present before undergoing surgery, or the medications being taken by patients, that the number of ATII cells present per lung area may be different. It is important to note that most patients smoke, which was visible in the samples as black areas.

ATII cell viability over a 24-hour period

Human ATII cells can maintain their phenotype in culture for at least 24 hours. This observation is very valuable because treatments in the presence of TGF-β, SARS-CoV-2 and/or plant extracts are performed during this time period.

The decrease in viability percentage observed after 12 hours is likely to be because at that time point, the sample was taken from the supernatant for counting, and not from the total (attached and suspension ATII cells), therefore alive cells which have attached to the plate were not considered, whereas dead cells would not attach meaning that a higher percentage of dead cells was observed in the supernatant. We conclude that these measurements should be done from the total of cells present in the assay. The results are also limited to one patient so may not represent cell viability in other patients. The method is limited to viability of nucleated cells and does not indicate if cells have differentiated. The method of counting cells also contains a relatively high degree of inaccuracy especially in primary cultures of cells where tissue residues remain and can easily be confounded with dead cells when stained with trypan blue. Removing cell debris and increasing the number of patients measured would improve the method.

Change in SPC expression in ATII cells 0h, 24h and 48h after defrosting

The results of SPC gene expression over time in culture show a remarkable drop in SPC expression in the first 24 hours of culture. Possible explanations could be that ATII cells could be dying or unhealthy, and therefore producing less SPC, or differentiating to non-SPC producing ATI cells. Total number of cells per extraction was higher in the 0h extractions and although defrosted cells were from the same patient, cells were taken from a different vial than those which had their RNA extracted after 24 and 48 hours so these factors could account for some of the difference observed. These results did not seem to support the results from the cell viability experiment using trypan blue however this could be due to patient variability or due to a certain percentage of cells changing phenotype, thus no longer producing SPC.

Cycle threshold (Ct) values were in the range of 23 and 29 for SPC expression at 0h however at 24- and 48-hours Ct values were in the range of 32 to 36 which is too high for control conditions to enable reliable comparison between control and treated conditions. This experiment was only performed in one patient, so cell viability is likely to vary considerably between patients. To address this problem, we increased the number of cells being used, reduced maximum incubation time from 48 hours to 24 hours and tested different plate coatings to reduce the range of Ct numbers by improving cell culture conditions to maintain ATII cell homeostasis. To improve this method cells would need to be defrosted at the same moment and divided into replicas of equal numbers for 0 hour, 24 hours, and 48 hours. More than one patient should be used, the number of cells in each condition could be increased to reduce Ct values and the number of replicas of each condition should be at least 3 in each condition in order to optimise the working conditions to obtain more reproducibility.

Effect of different culture dish coatings and cell number of SPC expression in ATII cells and conditions required for measurement of telomere length via HTQ-FISH techniques

ATII cells grow in suspension so either an insufficient number of cells were adhering to the preliminary culture plate sent for HTQ-FISH analysis or too many cells were becoming detached and lost during the stringent process. It was essential to find a coating that would allow a 24-hour treatment without promoting apoptosis or differentiation of cells and promote sufficient adhesion to the plate. Different cell culture plate coatings were tested for variability of SPC expression. Preliminary results showed differences between the coating tested with Matrigel being the more stable coating maintaining SPC expression. This is supported by a study that used gene expression profile analysis to compare freshly isolated human ATII cells growing on a Matrigel coating with those grown on a type I collagen coating over a 3 day period and found that Matrigel preserved ATII cell phenotype while collagen promoted differentiation (*30*). It is possible that there is a difference between cells remaining in suspension and those attached to the plate so the experiment could be repeated by extracting RNA from the supernatant and separately extracting RNA from the cells that remain attached to the plate to measure SPC expression enabling comparison. There is a clear decrease in SPC gene expression above 400,00 cells. In the case of 600,000 cells this could be explained by patient variability but with 800,000 cells of the same patient, SPC gene expression is also low. This could be because seeding such a high concentration of cells in 100 µl of cell culture medium could provide insufficient nutrients to cells and reduce their viability. A total of 200,000 cells per RNA extraction was sufficient to have SPC gene expression in two different patients and in on all coatings assayed. Results for the HTQ-FISH analysis are essential to determine the most suitable coating and number of cells required for future experiments.

Effect of TGF-β in ATII cells on SPC expression

This experiment was limited to only 2 replicas for each condition and 2 different concentrations of TGF-β because the number of cells extracted from patient 22 was low and did not allow for more. The results did show a tendency that SPC gene expression increased with an increasing concentration of TGF-β but to test whether or not this was actually the case or whether it was just due to the variability between replicas it would be necessary to repeat the experiment with more biological replicas. Another limitation of this experiment is that TGF-β is used to imitate COVID-19 infection in ATII cells but TGF-β alone is not representative of the cytokine storm.

CDC 2019-nCoV real-time RT-PCR diagnostic panel

This experiment demonstrated it was possible to infect ATII cells and for the virus to transcribe viral mRNA within cultured ATII cells. The results also showed that all viral titres assayed were sufficient to infect cells and be detected after a 24-hour incubation in cells from patient 27. The 2019-nCoV qPCR of patient 28 showed very high background noise confounding results so the experiment will need to be repeated.

SPC expression in SARS-CoV-2 infected ATII cells

Preliminary results show 3.5 ul titre of virus was the only concentration whereby cells were confirmed to be infected and SPC gene expression was obtained in both patients. In all cases, controls showed expression of SPC indicating that lack of expression or increase in SPC expression could be due to viral infection. Reproducibility of results between patients was very poor which could be due to patient variability or the baseline variability observed between biological replicas, however, to confirm this, the experiment would need to be repeated. It is necessary to infect cells with a concentration of virus that does not kill all cells within a 24-hour period so that SPC expression can be measured and compared between treatment groups.

During the process of inactivating the virus with hydrogen peroxide to take samples out of the BSL-3 laboratory, samples were left incubating in NYZol for the duration of this cycle (90 minutes) and due to a technical error, this cycle had to be repeated, therefore increasing the usual incubation time of 5 minutes in NYZol to 3 hours. This could have had led to degradation of the RNA in samples and could be why no SPC expression was observed in some conditions. Due to the poor reproducibility of results between patients this experiment should be repeated before selecting a viral titre for future experiments.

SPC expression in plant extract treated ATII cells

Because of the low overall range of relative SPC gene expression, differences in expression can be attributed to the usual degree of variation seen in the expression of SPC between biological replicas

which in previous experiments was up to 2.5 arbitrary units, and between cells from different patients and is unlikely to be due to properties of the plant extracts added as these differences were not reproduced. The lack of expression seen in some replicas was also not reproduced in other replicas, or in cells from another patient, so is likely to be due to a technical error at some point during the processing of the sample and unlikely to be due to toxicity of the plant extract. The results currently indicate that none of the plant extracts at a concentration of 0.4 ng/ml, or TGF-β at a concentration of 3 ng/ml, significantly alter SPC gene expression in ATII cells over a 24-hour period. The results also demonstrate that none of the plant extracts are highly toxic to ATII cells over a 24-hour treatment period. To further confirm these results more technical replicas of qPCRs should be performed to allow for statistical analysis. The results do not however indicate if either the plant extracts or TGF-β can cause a change in SPC gene expression in ATII cells in different concentrations. The assays would need to be repeated varying the concentrations of TGF-β and plant extracts to assess which concentrations do or do not have an effect. TGF-β has been used in these experiments to recapitulate COVID-19 disease but many other cytokines and chemokines are involved in COVID-19 disease, therefore using only TGF-β is not very representative of a SARS-CoV-2 infection and these experiments will need to be repeated using the virus instead of TGF-β. These experiments have, however, allowed us to optimise conditions, such as using fresh ATII cells instead of frozen cells, using a higher number of cells and using a plate coating in order to optimise cell viability and enable measurement of SPC gene expression.

Isolation of human fibroblasts from clinical lung samples

Initial experiments have been conducted by another member of the same laboratory group to measure expression of collagens 1 and 3, and fibronectin and how this expression changes in the presence of TGF-β and the plant extracts. Once experimental conditions have been established it will be possible to incubate fibroblasts and ATII cells together in the same well to see if infection and treatment of ATII cells produces a change in expression of collagens 1 and 3, and fibronectin.

Further research

This study has provided the preliminary steps for the conditions required to analyse changes in SPC gene expression in ATII cells under different treatment conditions. The conditions required to allow measuring both the change in SPC gene expression and measurement of telomere length by HTQ-FISH techniques within the same biological replica, have been assayed and definitive results from the CNIO are still pending. Further research will include treating ATII cells with plant extracts, subsequently infecting them with SARS-CoV-2 and measuring if there is any change in SPC gene expression. The supernatant of these ATII cells growing in suspension can be applied to a monolayer of fibroblasts so that, not only can the SPC gene expression be measured, but any change in fibrotic response can also

be indicated by measuring the relative expression of collagens 1 and 3, and fibronectin in fibroblasts, and whether or not there are plant extracts which are able to protect against a fibrotic response.

Conclusions

1: ATII cells were successfully extracted and purified from clinical lung samples and their purity was confirmed enzymatically.

2: ATII cell viability over a 24-hour period was shown not to decrease significantly and the total number of cells required to yield sufficient quantities of RNA to allow for retro-transcription and detection of SPC was determined to be 200,000 cells, however, this varied between patients.

3: The addition of 1ng/ml and 3 ng/ml TGF-β did not produce a significant difference in the expression of SPC in ATII cells compared to control conditions with 0 ng/ml TGF-β.

4: Preliminary results indicate that seeding 100,000 cells per well onto Matrigel and pooling 2 wells for RNA extraction were the optimal conditions to allow measurement of SPC expression, while the measurement of telomere length via HTQ-FISH techniques of cells remaining attached to the plates are still pending results from the CNIO.

5: Total metabolites of 4 plant extracts from *Marchantia* and total metabolites of 4 plant extracts from *Arabidopsis* showed no considerable change on the relative SPC expression in ATII cells compared to control conditions.

6: Preliminary results indicate 3.5 ul titre of virus in 100,000 cells seeded in 100 ul cell culture medium to be the optimal conditions for SARS-CoV-2 infection of ATII cells.

7: Primary human fibroblasts were successfully isolated and cultivated from clinical lung samples obtained from biopsies for future experiments.

Acknowledgments

I would like to thank Dr. Ana Villar Ramos and Dr. Ana Palanca and all members of the group I have been working with in the IBBTEC for their training, help and support during the last few months and the collaborators from the Institute of Biomedical Research of Barcelona (IIBB-CSIC) and the Spanish National Cancer Research Centre (CNIO) for their help on this project. I´d also like to thank Dr. Yelina Ortiz Pérez for the infection of cells with SARS-CoV-2.

Bibliography

1. W. H. Organisation.
2. N. Zhu *et al.*, A Novel Coronavirus from Patients with Pneumonia in China, 2019. *N Engl J Med* **382**, 727-733 (2020).
3. S. A. A. Mamun, R. Jahan, Q. T. Islam, T. Nazrin, K. Shajalal, Rationale of Using Common Antifibrotic Therapy in Post COVID
   Fibrosis. *Journal of Medicine* **22**, 5 (2021).
4. A. Vitiello, C. Pelliccia, F. Ferrara, COVID-19 Patients with Pulmonary Fibrotic Tissue: Clinical Pharmacological Rational of Antifibrotic Therapy. *SN Compr Clin Med*, 1-4 (2020).
5. M. Carcaterra, C. Caruso, Alveolar epithelial cell type II as main target of SARS-CoV-2 virus and COVID-19 development via NF-Kb pathway deregulation: A physio-pathological theory. *Med Hypotheses* **146**, 110412 (2021).
6. B. S. Johnson, M. Laloraya, A cytokine super cyclone in COVID-19 patients with risk factors: the therapeutic potential of BCG immunization. *Cytokine Growth Factor Rev* **54**, 32-42 (2020).
7. A. Zumla, D. S. Hui, E. I. Azhar, Z. A. Memish, M. Maeurer, Reducing mortality from 2019-nCoV: host-directed therapies should be an option. *Lancet* **395**, e35-e36 (2020).
8. A. Vafaeinezhad, M. R. Atashzar, R. Baharlou, The Immune Responses against Coronavirus Infections: Friend or Foe? *Int Arch Allergy Immunol*, 1-14 (2021).
9. S. Mulugeta, M. F. Beers, Surfactant protein C: its unique properties and emerging immunomodulatory role in the lung. *Microbes Infect* **8**, 2317-2323 (2006).
10. A. G. Harrison, T. Lin, P. Wang, Mechanisms of SARS-CoV-2 Transmission and Pathogenesis. *Trends in Immunology*, (2020).
11. J. N. Zou *et al.*, The characteristics and evolution of pulmonary fibrosis in COVID-19 patients as assessed by AI-assisted chest HRCT. *PLoS One* **16**, e0248957 (2021).
12. J. Prakash, P. K. Bhattacharya, S. Priye, N. Kumar, Post-COVID-19 Pulmonary Fibrosis: A Lifesaving Challenge. *Indian J Crit Care Med* **25**, 104-105 (2021).
13. B. Kayarat, P. Khanna, S. Sarkar, Pulmonary Fibrosis in COVID-19 Recovered Patients: Problem and Potential Management. *Indian J Crit Care Med* **25**, 242-244 (2021).
14. N. C. Henderson, F. Rieder, T. A. Wynn, Fibrosis: from mechanisms to medicines. *Nature* **587**, 555-566 (2020).
15. T. Espeland, I. G. Lunde, B. H Amundsen, L. Gullestad, S. Aakhus, Myocardial fibrosis. *Tidsskr Nor Laegeforen* **138**, (2018).
16. D. Pohlers *et al.*, TGF-beta and fibrosis in different organs - molecular pathway imprints. *Biochim Biophys Acta* **1792**, 746-756 (2009).
17. R. Sanchez-Vazquez, A. Guío-Carrión, A. Zapatero-Gaviria, P. Martínez, M. A. Blasco, Shorter telomere lengths in patients with severe COVID-19 disease. *Aging (Albany NY)* **13**, 1-15 (2021).
18. S. Piñeiro-Hermida *et al.*, Telomerase treatment prevents lung profibrotic pathologies associated with physiological aging. *J Cell Biol* **219**, (2020).
19. T. Liu, F. G. De Los Santos, S. H. Phan, The Bleomycin Model of Pulmonary Fibrosis. *Methods Mol Biol* **1627**, 27-42 (2017).
20. D. M. Pott, S. Osorio, J. G. Vallarino, From Central to Specialized Metabolism: An Overview of Some Secondary Compounds Derived From the Primary Metabolism for Their Role in Conferring Nutritional and Organoleptic Characteristics to Fruit. *Front Plant Sci* **10**, 835 (2019).
21. I. Koch, J. Nöthen, E. Schleiff, Modeling the Metabolism of Arabidopsis thaliana: Application of Network Decomposition and Network Reduction in the Context of Petri Nets. *Front Genet* **8**, 85 (2017).
22. T. Ghrairi *et al.*, New Insights into and Updates on Antimicrobial Agents from Natural Products. *Biomed Res Int* **2019**, 7079864 (2019).

23. S. Nandy, A. Dey, Bibenzyls and bisbybenzyls of bryophytic origin as promising source of novel therapeutics: pharmacology, synthesis and structure-activity. *Daru* **28**, 701-734 (2020).
24. P. Procházková Schrumpfová, Š. Schořová, J. Fajkus, Telomere- and Telomerase-Associated Proteins and Their Functions in the Plant Cell. *Front Plant Sci* **7**, 851 (2016).
25. C. Chang, J. L. Bowman, E. M. Meyerowitz, Field Guide to Plant Model Systems. *Cell* **167**, 325-339 (2016).
26. M. Shimamura, Marchantia polymorpha: Taxonomy, Phylogeny and Morphology of a Model System. *Plant Cell Physiol* **57**, 230-256 (2016).
27. S. Hosseini, M. Imenshahidi, H. Hosseinzadeh, G. Karimi, Effects of plant extracts and bioactive compounds on attenuation of bleomycin-induced pulmonary fibrosis. *Biomed Pharmacother* **107**, 1454-1465 (2018).
28. A. Canela, E. Vera, P. Klatt, M. A. Blasco, High-throughput telomere length quantification by FISH and its application to human population studies. *Proc Natl Acad Sci U S A* **104**, 5300-5305 (2007).
29. F. I. Uzel, S. İliaz, F. Karataş, B. Çağlayan, COVID-19 Pneumonia and Idiopathic Pulmonary Fibrosis: A Novel Combination. *Turk Thorac J* **21**, 451-453 (2020).
30. H. Morales Johansson, D. R. Newman, P. L. Sannes, Whole-genome analysis of temporal gene expression during early transdifferentiation of human lung alveolar epithelial type 2 cells in vitro. *PLoS One* **9**, e93413 (2014).